RSC Advances

ROYAL SOCIETY OF CHEMISTRY

www.rsc.org/advances

RSC Advances

COMMUNICATION

Highly dispersed Ag nanoparticles embedded in alumina nanobelts as excellent surface-enhanced Raman scattering substrates

Received 00th January 20xx,
Accepted 00th January 20xx

DOI: 10.1039/x0xx00000x

www.rsc.org/

Zhifeng Dou, *[,a] Chao Cui, [a] Yuhong Feng, [a] Yong Chen[a] and Guizhen Wang*[,b]

Nearly monodispersed Ag nanoparticles embedded in alumina nanobelts were fabricated with a template method by integrating facile coordination polymerization with atomic layer deposition (ALD) technique. The composite nanobelts with specific hierarchical micro/nano-structure showed superior SERS properties for R6G probe molecule.

Surface-enhanced Raman scattering (SERS) technology has been most intensively exploited in many areas of chemical analysis, biological analysis, medical detection and other molecule identification applications due to its high sensitivity, rapid response and fingerprint effect.[1-3] In comparison to normal Raman spectroscopy, SERS utilizes the collective plasmon resonances arising from localized surface plasmon resonances (LSPR) of active substrate, commonly referred to as "hot spots". The sensitivity and intensity of LSPR strongly depend on the size, shape and roughness of the substrates, which in turn affect the intensity of the SERS signal.[4, 5]

It is generally acknowledged that LSPR is most easily observed on or near roughened surfaces and nanoparticles of noble metal.[6-10] Therefore, many great efforts have been made to fabrication noble metal-based SERS-active substrate.[11-14] However, from an application point of view, a prominent SERS substrate is required not only to be high enhancement factor but highly stable, repeatable, cheap, and facile to be prepared.[15] So a great challenge that remains is to develop effective, inexpensive and feasible ways to organize the nanoscale particles into functional structures or devices to meet the practical application requirements for SERS substrate.[16-19]

Herein, we demonstrate a facile template method to fabricate nearly monodispersed Ag nanoparticles embedded into the inner wall of alumina nanobelts (Ag/Al_2O_3) by integrating facile coordination polymerization with atomic layer deposition (ALD) technique. Firstly, One-dimensional twisted Ag-melamine nanobelts coordination polymers (CPs) were obtained by aqueous solution coordination polymerization of silver nitrate and melamine (MA) in room temperature. The clean glass substrates were drop-coated with the as-prepared AgMA CPs and subsequently put into deposition chamber of ALD to deposit alumina layer on the surface of AgMA CPs after drying in oven. The final products of twisted alumina nanobelts embedded by relatively uniform and highly dispersed silver nanoparticles could be acquired by calcining as-prepared ALD products in nitrogen atmosphere. The above synthetic process is shown schematically in Fig. 1 and detailed synthetic process can refer to experiment section in the electronic supplementary information (ESI†).

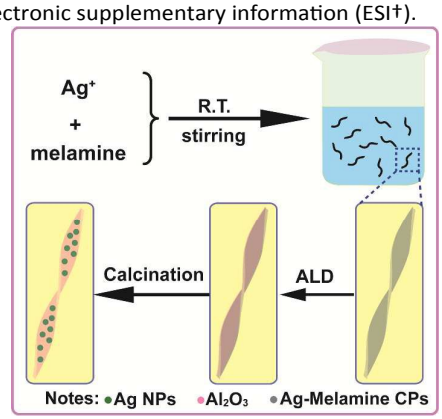

Fig. 1 Schematic illustration of fabricating the twisted Ag/Al_2O_3 composite nanobelts.

It's well known that coordination polymers (CPs) can organize metal ions and small organic molecules building blocks into diverse functional supramolecular architectures through primary metal-ligand coordination bonds and multiple weak interactions such as hydrogen bonding, π-π stacking interactions and van der Waals forces.[20-24] In this method, milky AgMA CPs could be obtained by facile aqueous solution reaction in room temperature. The morphologies of the milky

[a] State Key Lab of Marine Resource Utilization in South China Sea and Center of Analysis and Testing (CAT), College of Materials and Chemical Engineering, Hainan University, Haikou, 570228, P. R. China. Fax & Tel: 86-0898-66168037; E-mail: douzf@hainu.edu.cn
[b] Key Laboratory of Tropical Biological Resources of Ministry of Education, College of Materials and Chemical Engineering, Hainan University, Haikou, 570228, P. R. China. Fax & Tel: 86-0898-66168172; E-mail: wangguizhen0@hotmail.com
Electronic Supplementary Information (ESI) available: Electronic Supplementary Information (ESI) available: SEM images, EDX results, Raman spectra, TG and DTG curves, as well as experimental details. See DOI: 10.1039/x0xx00000x

AgMA CPs were examined by scanning electron microscopy (SEM) and transmission electron microscopy (TEM). As shown in Fig. 2a, the milky precursor products were twisted nanobelts in large scale (Fig. S1, ESI†). SEM and TEM results revealed that the width and thickness of the nanobelts were about 50~200 nm and 20~50 nm, respectively. Moreover, the helical pitch was closely related to the width of the nanobelts, namely, the larger width, the longer helical pitch (Fig 2b).

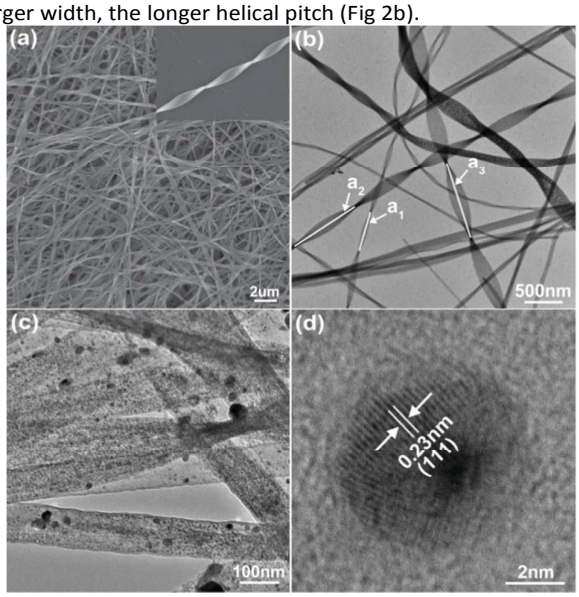

Fig. 2 SEM image (a) and TEM image (b) of the milky precursor products; TEM image (c) and single silver nanoparticle HRTEM image (d) of the final products.

Energy-dispersive X-ray (EDX) analysis showed that the Ag/N atomic ratio in these twisted nanobelts was about 1:7 (Fig. S2, ESI†), which was consistent with the results reported in the literature attributed to molecular formula $\{Ag(C_3H_6N_6)NO_3\}_n$. In this CPs, the MA and Ag building blocks were connected through Ag-N bonds forming MA-Ag-M-Ag chains. However, the N-Ag-N bonds in such complexes were not truly linear, leading to a helical conformation rather than a linear chain.[25] At the same time, hydrogen bonding between the adjacent chains promoted the one-dimensional twisted architecture.[26]

The thermal decomposition behavior of the AgMA CPs was examined by thermogravimetric analysis (TGA). The results showed that there were three main weight loss stages (Fig. S3, ESI†). The first 2% weight loss before 200 °C was mainly due to the elimination of absorbed water and crystallization water of the sample. Subsequently, there was a distinct weight loss between 200 °C and 325 °C, which accounted for 51% of the total weight. The weight loss was ascribed to the release of gas phase products during organic ligand pyrolysis.[27] With the temperature raised further, the weight loss rate decreased gradually and the weight tended to be constant.

The representative microstructure and morphology of the final products calcined in nitrogen atmosphere were characterized by TEM. The results (Fig. 2c, d) showed that the twisted nanobelts morphology remained well after annealing and the nanobelts were decorated with silver nanoparticles. The enlarged TEM image (Fig. S4a, ESI†) revealed that the size (D) distribution of silver nanoparticles was very narrow and the statistic analysis (Fig. S4b, ESI†) showed the particles size was mainly concentrated in the range of 5 to 9 nm. The control experiment without ALD pretreatment was also carried out (detailed in ESI†) and irregular microparticles instead of the composite twisted nanobelts were obtained (Fig. S4c, ESI†). This indicated that ALD pretreament was requisite step to obtain the composite twisted nanobelts. ALD is a versatile coating technique that produces films with uniform and conformal layer by a sequence of self-limiting reactions of gas-phase precursor molecules.[28] During the ALD process, the amorphous alumina thin films with excellent conformality and confinement effect were introduced into the precursor surface. The films could inhibit the agglomeration of silver nanoparticles in the following calcination process and enhance the stability of the nanoparticles.

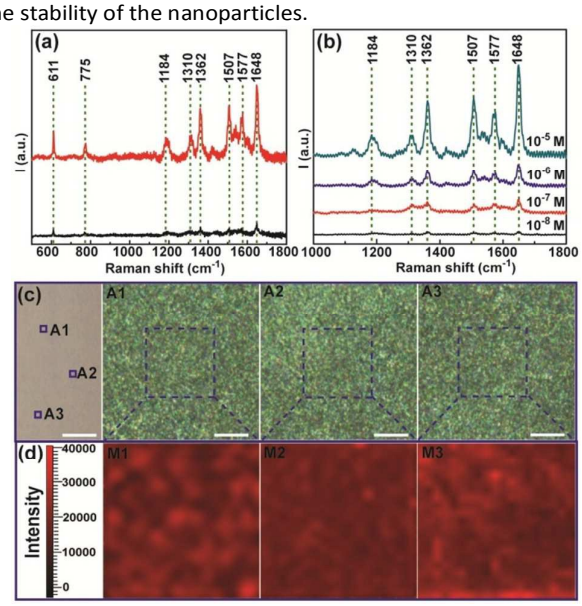

Fig. 3 Raman spectra of R6G molecules collected in different conditions: (a) 10^{-6} M R6G molecules on the as-prepared Ag/Al_2O_3 substrates (red spectrum) and 0.1 M R6G molecules on glass slide substrates (black spectrum); (b) R6G molecules with different concentrations on as-prepared Ag/Al_2O_3 substrates. (c) Optical photograph (left) and white light microscope images of the as-prepared substrate in corresponding area A1, A2 and A3, scale bar: 10 mm and 10 μm, respectively; (d) Corresponding SERS maps (611 cm^{-1} signal intensities to baseline, 20×20 μm^2, step size 1 μm) of 10^{-6} M R6G molecules in selected areas of the as-prepared substrate.

The performance of the as-prepared SERS-active substrates Ag/Al_2O_3 nanobelts was characterized with Rhodamine 6G (R6G) used as the probe molecule (detailed in ESI experiment sections). The characteristic Raman spectrum of probe molecules on as-prepared SERS-active substrates is showed in Figure 3a (red spectrum).

In order to quantitatively evaluate the SERS enhancement ability of as-prepared SERS-active substrates, rough calculations of Raman enhancement factors (EFs) are conducted with employing the formula $EF = (I_{SERS} / I_{ref}) \times (C_{ref} / C_{SRES})$, where I_{SERS} is the enhanced Raman intensity of the absorbed R6G molecules on the SERS substrates, I_{ref} is the

normal Raman intensity of on the blank glass slide, and C_{SRES} and C_{ref} are the concentrations of molecules in the SERS substrate and blank glass slide, respectively.[29]

Figure 3a reveals Raman spectra of 10^{-6} M and 0.1 M R6G molecules collected on as-prepared Ag/Al_2O_3 substrate (red spectrum) and reference glass slide (black spectrum). The SERS intensity of the band at 611 cm^{-1} was used for the calculations. The calculation results show that the EF of Ag/Al_2O_3 nanobelts was estimated to ca. 5.2×10^6 by the formula.

The limit of detection (LOD) for R6G molecules on the nanobelts was determined by measuring SERS spectra of R6G molecules on the nanobelts substrates with the varied concentrations from 10^{-5} to 10^{-8} M. All the measurements were conducted under identical experimental conditions. As shown in Fig. 3b, the spectral intensity of the characteristic vibrations in the Raman shift between 1000 and 1800 cm^{-1} decreases gradually with decreasing of the concentration from 10^{-5} to 10^{-8} M. However, the characteristic Raman signals of R6G molecules were still evident as detected concentration down to 10^{-8} M.

Figure 3c showed that the prepared substrate was highly uniform in the visual and white light microscope observation. To illustrate the homogeneity of the prepared substrate of the SERS signal, Raman mappings of different areas (Fig 3c, A1, A2 and A3) selected randomly were taken on an area of 20 × 20 μm^2 with a step of 1 µm basing on 611 cm^{-1} signal intensities to baseline of 10^{-6} M R6G. The SERS mapping results (Fig. 3d) shows that the SERS signal intensities tend to be uniform in large randomly selected areas, indicating that the fabricated Ag/Al_2O_3 nanobelts substrates were uniform and had highly reproducible SERS performance.

The above SERS characterization results revealed that the as-prepared Ag/Al_2O_3 nanobelts possessed excellent enhancement performances for R6G probe molecule. Based on structure-property correlations, excellent SERS abilities might be related to the specific microstructure. In this substrate microstructure, silver nanoparticles as active components were highly dispersed in alumina nanobelts. And so each silver nanoparticle was equivalent to the formation of shell-isolated SERS mode, which could greatly enhance detection sensitivity of SERS.[30] The thin alumina layer could enhance the polar interaction between the analyte molecules and the substrates by modifying the surface chemistry of substrates.[31] The control samples without ALD pretreatment were evaluated under the same condition and the results showed that the Raman signal intensities were significantly smaller than them of as-prepared Ag/Al_2O_3 nanobelts (Fig. S5, ESI†).

Comparing to micrometer scale particles, nanoparticles had more exposed active surface, on which more plasmon resonances could be induced in the same irradiation area. Moreover, nanometer scale hot spots were greatly beneficial to obtain a uniform SERS signal due to a large number of hot spots contained per square micron. In addition, the morphologies of Ag nanoparticles were not typical spherical but irregular anisotropic structure with sharp edges and vertices, which had greater enhancement factors.[32] At the same time, there were a large number of gaps between the nanoparticles and these gaps could be acted as hot spots for Raman enhancement.[33-35]

In summary, nearly monodispersed Ag nanoparticles embedded into the inner wall of alumina nanobelts (Ag/Al_2O_3) were obtained with a new template method by integrating facile coordination polymerization with atomic layer deposition (ALD) technique. In this synthesis strategy, inorganic silver source was dispersed uniformly in the precursor by the formation of AgMA CPs and then Ag/Al_2O_3 nanobelts could be obtained by using excellent conformality and confinement effects of alumina thin films during the following calcination process. In SERS applications, the nanobelts showed excellent SERS performances for R6G probe molecule, including high enhancement factors, low detection limit and excellent substrate homogeneity. The specific microstructure of the composite nanobelts with a large number of active hot spots was the key to their high SERS performance.

Acknowledgements

The authors greatly appreciate the financial support from National Natural Science Foundation of China (11564011, 51362010, 51362009) and the Natural Science Foundation of Hainan Province (20152018, 514212).

Notes and references

1 H. Tang, G. Meng, Q. Huang, Z. Zhang, Z. Huang and C. Zhu, *Adv. Funct. Mater.*, 2012, **22**, 218-224.
2 Z. Dai, G. Wang, X. Xiao, W. Wu, W. Li, J. Ying, J. Zheng, F. Mei, L. Fu, J. Wang and C. Jiang, *J. Phys. Chem. C*, 2014, **118**, 22711-22718.
3 S. Schlücker, *Angew. Chem. Int. Ed.*, 2014, **53**, 4756-4795.
4 Q. Yu, P. Guan, D. Qin, G. Golden and P. M. Wallace, *Nano Lett.*, 2008, **8**, 1923-1928.
5 K.-S. Lee and M. A. El-Sayed, *J. Phys. Chem. B*, 2006, **110**, 19220-19225.
6 Y. Su, Q. He, X. Yan, J. Fei, Y. Cui and J. Li, *Chem. Eur. J.*, 2011, **17**, 3370-3375.
7 K. J. Khajehpour, T. Williams, L. Bourgeois and S. Adeloju, *Chem. Commun.*, 2012, **48**, 5349-5351.
8 S. L. Kleinman, R. R. Frontiera, A.-I. Henry, J. A. Dieringer and R. P. Van Duyne, *Phys. Chem. Chem. Phys.*, 2013, **15**, 21-36.
9 C. L. Haynes, A. D. McFarland and R. P. V. Duyne, *Anal. Chem.*, 2005, **77**, 338 A-346 A.
10 L. Tong, T. Zhu and Z. Liu, *Chem. Soc. Rev.*, 2011, **40**, 1296-1304.
11 J. Fei, Y. Cui, A. Wang, P. Zhu and J. Li, *Chem. Commun.*, 2010, **46**, 2310-2312.
12 S. Y. Lee, S.-H. Kim, M. P. Kim, H. C. Jeon, H. Kang, H. J. Kim, B. J. Kim and S.-M. Yang, *Chem. Mater.*, 2013, **25**, 2421-2426.
13 Q. Zhang, Y. H. Lee, I. Y. Phang, C. K. Lee and X. Y. Ling, *Small*, 2014, **10**, 2703-2711.
14 L. Zhang, T. Liu, K. Liu, L. Han, Y. Yin and C. Gao, *Nano Lett.*, 2015, **15**, 4448-4454.
15 B. Zhang, H. Wang, L. Lu, K. Ai, G. Zhang and X. Cheng, *Adv. Funct. Mater.*, 2008, **18**, 2348-2355.
16 J. Fei and J. Li, *Adv. Mater.*, 2015, **27**, 314-319.
17 Y. Lu, G. L. Liu and L. P. Lee, *Nano Lett.*, 2005, **5**, 5-9.
18 N. A. Cinel, S. Bütün, G. Ertaş and E. Özbay, *Small*, 2013, **9**, 531-537.

19 Z. Dou, C. Cao, Y. Chen and W. Song, *Chem. Commun.*, 2014, **50**, 14889-14891.
20 Y.-H. Li, D. Sun, G.-G. Luo, F.-J. Liu, H.-J. Hao, Y.-M. Wen, Y. Zhao, R.-B. Huang and L.-S. Zheng, *J. Mol. Struct.*, 2011, **1000**, 85-91.
21 W. L. Leong and J. J. Vittal, *Chem. Rev.*, 2010, **111**, 688-764.
22 C. Li, K. Deng, Z. Tang and L. Jiang, *J. Am. Chem. Soc.*, 2010, **132**, 8202-8209.
23 A. M. Spokoyny, D. Kim, A. Sumrein and C. A. Mirkin, *Chem. Soc. Rev.*, 2009, **38**, 1218-1227.
24 Y. Shen, J. Wang, U. Kuhlmann, P. Hildebrandt, K. Ariga, H. Möhwald, D. G. Kurth and T. Nakanishi, *Chem. Eur. J.*, 2009, **15**, 2763-2767.
25 J. Fei, L. Gao, J. Zhao, C. Du and J. Li, *Small*, 2013, **9**, 1021-1024.
26 K. Sivashankar, A. Ranganathan, V. R. Pedireddi and C. N. R. Rao, *J. Mol. Struct.*, 2001, **559**, 41-48.
27 Z. S. Hang, L. H. Tang, F. Y. Ju, B. Zhou and S. J. Ying, *J. Anal. Sci.*, 2011, **27**, 279-283.
28 C. Marichy, M. Bechelany and N. Pinna, *Adv. Mater.*, 2012, **24**, 1017-1032.
29 E. C. Le Ru, E. Blackie, M. Meyer and P. G. Etchegoin, *J. Phys. Chem. C*, 2007, **111**, 13794-13803.
30 X. Zhang, J. Zhao, A. V. Whitney, J. W. Elam and R. P. Van Duyne, *J. Am. Chem. Soc.*, 2006, **128**, 10304-10309.
31 J. F. Li, Y. F. Huang, Y. Ding, Z. L. Yang, S. B. Li, X. S. Zhou, F. R. Fan, W. Zhang, Z. Y. Zhou, Y. Wu de, B. Ren, Z. L. Wang and Z. Q. Tian, *Nature*, 2010, **464**, 392-395.
32 L. A. Lane, X. Qian and S. Nie, *Chem. Rev.*, 2015, **115**, 10489-10529.
33 H. Xu, J. Aizpurua, M. Käll and P. Apell, *Physical Review E*, 2000, **62**, 4318-4324.
34 H. H. Wang, C. Y. Liu, S. B. Wu, N. W. Liu, C. Y. Peng, T. H. Chan, C. F. Hsu, J. K. Wang and Y. L. Wang, *Adv. Mater.*, 2006, **18**, 491-495.
35 Q. Fu, Z. Zhan, J. Dou, X. Zheng, R. Xu, M. Wu and Y. Lei, *ACS Appl. Mater. Inter.*, 2015, **7**, 13322-13328.

Table of Content

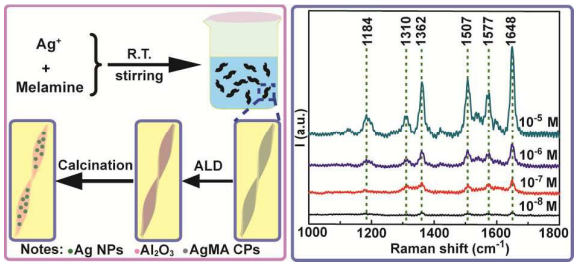

The Ag/Al_2O_3 composite nanobelts with nearly monodispersed Ag nanoparticles embedded in alumina nanobelts show excellent SERS performances for R6G probe molecule.